Gas Permeation Resistance of Various Grades of Perfluoroalkoxy–Polytetrafluoroethylene Copolymers

L. Monson, Sung In Moon, C. W. Extrand

Entegris, Inc., 3500 Lyman Blvd., Chaska, MN 55318

ABSTRACT: The permeation resistance of various grades of perfluoroalkoxy (PFA)/polytetrafluoroethylene (PTFE) copolymers was tested. Specimens were compression molded using two different cooling techniques: a faster one (ice water quench) and a slower one (press cooled). Permeability, diffusion, and solubility coefficients were measured for hydrogen, nitrogen, and oxygen gases. The slow cooled samples always showed much better permeation resistance than those cooled quickly, demonstrating that process can be as important as polymer grade in determining the ultimate permeation resistance of PFA. For a given cooling method, molecular mass (chain length) had no appreciable affect on the permeation resistance. On the other hand, PFA grades with increased comonomer content appeared to have slightly diminished permeation resistance whereas grades with PTFE filler had better permeation resistance. Differences in permeation resistance were attributed to variation in crystallinity arising from differences in molecular architecture and processing. © 2008 Wiley Periodicals, Inc. J Appl Polym Sci 111: 141–147, 2009

Key words: diffusion; fluoropolymers; polytetrafluoroethylene (PTFE) copolymer; perfluoroalkoxy (PFA); structure-property relations

INTRODUCTION

Fluoropolymers are the materials of choice for many materials integrity management applications. They provide a unique combination of toughness, purity, and chemical inertness. Among the melt-processable fluoropolymers, polytetrafluoroethylene (PTFE)–perfluoroalkoxy (PFA) copolymers, often abbreviated simply as PFA, have the highest service temperature and therefore have been used broadly in semiconductor fabrication.[1,2] In recent years, new grades of PFA have been introduced that improve fatigue life or permeation resistance. In general, these improvements come from changing the type of comonomer, increasing its content, or adding permeation resistant fillers. Because increasing comonomer content reduces crystallinity and increases ductility, the price to pay for better fatigue life performance may be reduced permeation resistance.

A great deal is known about the purity, mechanical, and thermal properties of PTFE and its copolymers,[3–5] but less information is available regarding their permeation characteristics. Although some permeation studies have been performed,[6–13] many have focused on fluoropolymers for membrane applications.[11–13] Because PFA is a semicrystalline polymer, its properties can be strongly affected by the processing conditions. Therefore, this article explores the influence of molecular architecture and processing on the permeation resistance of various grades of PFA.

EXPERIMENTAL

Materials and methods

Five grades of DuPont Teflon® PFA were selected for the study: 440HP, 450HP, 451HPJ, 950HP+, and 951HP+. The grades were chosen to provide a wide range of polymer structure and morphology. For example, 440HP and 450HP differ in their molecular mass (or chain length); 950HP+ has higher comonomer content than 440HP or 450HP; both 451HPJ and 951HP+ contain PTFE filler.

Specimens were compression-molded at 343°C (650°F) using a PHI Bench Design, Hydraulic Compression Press. A specified amount of resin was weighed out for desired film thickness, poured into the center of a brass plaque mold and then sandwiched between thin aluminum sheets. This sandwich was placed on the preheated lower platen of the press and brought into contact with the top platen and held for 5 min, after which a load of 1700 kg was applied for 2 min then increased to 3400 kg for 2 min.

At this point, two different methods of cooling were employed that produced quite different

Correspondence to: C. W. Extrand (chuck_extrand@entegris.com).

polymer morphology and permeation resistance for a given grade. These methods are as follows:

Ice water quench: The sandwich was quickly cooled by dropping it in ice water for approximately 1 min, and then placing it between two chilled aluminum blocks for 10–15 min.

Press cooled: The sandwich was left in the press (under 3400 kg load). The heat was turned off and the sandwich was allowed to cool slowly overnight with the platens intact (approximately 16–18 h).

Melt flow rates were measured using a Kayness Galaxy I Melt Flow Indexer. The die radius was 0.1048 cm, and its length was 0.80 cm. Specimens were cut into small pieces, loaded into to a 372°C melt indexer and allowed to preheat for 6 min, and then a 5000 g load was applied. Results were reported as dg/min. Triplicate measurements were made for each material.

Melt temperatures (T_m) and melt enthalpies (ΔH) of the various films were determined using differential scanning calorimetry (Perkin–Elmer DSC7). Samples ranging in mass from 4 to 8 mg were cut from specimens, heated from 50°C (122°F) to 350°C (662°F), cooled from 350 to 50°C, and then heated again from 50 to 350°C at a rate of 10°C/min (18°F/min). Triplicate DSC scans were performed for each material. Using the software resident in the DSC7, the resulting DSC scans were analyzed.

The type and content of comonomer were evaluated using a method reported in the literature.[14] Thin films were compression-molded from the PFA 440HP, 450HP, 451 HPJ, 950HP+, and 951HP+ resins at 350°C. (The process was the same as described earlier for permeation specimens, but the IR samples were thinner, usually less than 0.13 mm.) Fourier transfer infrared (FTIR) spectra were taken with a Nicolet Nexus 470 and used to determine the type and quantity of perfluoroalkyl vinyl ether (PAVE) comonomer present in these PTFE copolymers. A peak at 995 cm^{-1} represents the presence of perfluoro(propyl vinyl ether) (PPVE) comonomer and a peak at 1090 cm^{-1} represents perfluoro(ethyl vinyl ether) (PEVE) comonomer. Mass fractions of comonomer were calculated by dividing the height of these peaks by the height of an internal reference peak at 2365 cm^{-1} and then multiplying by the appropriate conversion factor: $f = 0.94$ for the PPVE and $f = 1.33$ for the PEVE. [These conversions were taken from the Ref. 14 and originally obtained from calibration with 19F nuclear magnetic resonance (NMR) spectroscopy data.] Molar masses of the PAVE and tetrafluoroethylene (TFE) monomers used to determine mole fractions were $M_{PPVE} = 266$ g/mol, $M_{PEVE} = 216$ g/mol, and $M_{TFE} = 100$ g/mol.

The permeant gases (hydrogen, oxygen, and nitrogen) were industrial grade, (Toll, Minneapolis, MN). The gas permeation apparatus consisted of a sample holder inside of a temperature-controlled chamber, a series of valves, an upstream ballast tank, a pressure transducer (300 psi Heise PM Digital Indicator) for the upstream gas, and a downstream solid-state manometer (10 Torr MKS Baratron Type 627B). The apparatus was constructed from stainless steel. Connections were made by welding or with VCR flanges to minimize leaks. Data acquisition and control were performed remotely with a personal computer.

Permeation was measured according to standard manometric procedures as described below.[15,16] A circular specimen with a diameter of 4.6 cm and an effective area (A) of 13.7 cm^2 was placed in the gas permeation apparatus. The apparatus was pumped down to approximately 20 mTorr and held overnight to remove volatile constituents from the apparatus as well as from the specimen. The next day, the apparatus was leak tested. If the leak rate was sufficiently low, then the upstream side of the apparatus was charged with the permeant gas. After pressure and temperatures were allowed to equilibrate for a few minutes, the test was started. The downstream pressure rise (Δp_l) was recorded with the passage of time [temperature and upstream pressure (Δp) also were monitored over the duration of the experiment to assure their constancy].

In a previous study, the mass-transfer characteristics of PFA were shown to be independent of thickness for sufficiently thick specimens.[10] Therefore, all permeation measurements were taken from thicknesses between 0.25 and 0.50 mm using three gas pressures (1, 2, and 3 atm for hydrogen and 2, 4, and 6 for oxygen and nitrogen) at 25°C (77°F).

Analysis

The crystalline mass fraction (x_c) was calculated as[17]

$$x_c = \frac{\Delta H}{H_f} \tag{1}$$

where ΔH is the measured melting enthalpy, and H_f is the melting enthalpy of the polymer in a 100% crystalline state. The mass fraction of the PAVE comonomer (x_{PAVE}) in the PTFE copolymers was determined from FTIR spectroscopy by multiplying a ratio of the intensity of comonomer absorption peak (I_{PAVE}) to an internal reference peak from the CF$_2$ combination mode (I_{ref}) by a correction factor (f),[14]

$$x_{PAVE} = \frac{I_{PAVE}}{I_{ref}} f. \tag{2}$$

In turn, the mole fraction PAVE comonomer (v_{PAVE}) in PTFE copolymers was estimated as

$$v_{PAVE} = \frac{x_{PAVE}/M_{PAVE}}{x_{PAVE}/M_{PAVE} + (1 - x_{PAVE})/M_{TFE}}, \quad (3)$$

where M_{TFE} and M_{PAVE} are the molar masses of TFE and the specific PAVE comonomer. The mass fraction of PTFE in PFA/PTFE blends can be resolved from the following expression

$$x_{PTFE} = 1 - x_{PFAb}/x_{PFAj}, \quad (4)$$

where the numerator (x_{PFAb}) is the mass fraction of the PAVE comonomer in the PTFE filled PFA blend (451HPJ or 951HP+) and the denominator (x_{PFAj}) is the mass fraction of the PAVE comonomer in the corresponding unfilled PFA (450HP or 950HP+).

Gases permeate through homogeneous materials by first dissolving and then diffusing.[18] The downstream pressure rise (Δp_l) of the permeant can be converted to an equivalent volume of gas (V) at standard temperature and pressure (STP),

$$V = (\Delta p_1/\Delta p_o)(T_o/T)V_s, \quad (5)$$

where T is the measurement temperature, V_s is the volume of the downstream side of the permeation apparatus, T_o is standard temperature ($0°C = 273$ K) and Δp_o is standard pressure (=1 atm or 76 cmHg). The volume (V) of gas that permeates through a film with time (t) under steady state conditions depends on the permeability coefficient (P), as well as film thickness (B), film area (A), and the applied upstream pressure (Δp),[5,19]

$$V = \frac{PA\Delta pt}{B}. \quad (6)$$

The time required for a permeant to break though a film (t_b) depends on the film thickness (B) and the diffusion coefficient of the material,

$$t_b = \frac{B^2}{6D}. \quad (7)$$

Solubility coefficients were calculated from permeability and diffusion coefficients as,

TABLE I
Melt Flow Properties for Different PFA Resins and Films

Grade	Resin (dg/min)	Film (dg/min)
440HP	16.0 ± 0.1	16.0 ± 1
450HP	1.74 ± 0.03	1.86 ± 0.16
451HPJ	2.03 ± 0.04	2.12 ± 0.23
950HP+	1.93 ± 0.03	2.21 ± 0.41
951HP+	1.81 ± 0.03	2.04 ± 0.30

$$S = \frac{P}{D} \quad (8)$$

RESULTS AND DISCUSSION

Flow properties are summarized in Table I. Melt flow rates were performed on the resin and on 0.25 mm compression molded films prior to testing to ensure that processing had not degraded them. All MFR values for both resins and films fell within the supplier specified ranges.

Thermal properties of the various PFA films are listed in Table II. Melt temperatures (T_m) ranged from 283°C (541°F) to 328°C (622°F) and melt enthalpies from 13 to 29 J/g. These values generally agreed with previously reported ones.[5,10] Corresponding crystalline mass fractions (x_c) were calculated from eq. (1) using a ΔH_f value of 67 J/g[17]; x_c values fell between 19 and 43%.

Figure 1 shows representative DSC thermograms of two PFA grades used in this study. It is obvious the cooling method strongly affects the melting behavior. Ice-quenched specimens showed more melting at lower temperature and had less crystallinity than their press cooled counterparts. Whereas, the ice-quenched specimens were cooled in less than 1 min, the press cooled one had much more time to crystallize. The initial cooling rate during press cooling was slow, approximately 1.5°C/min, and continued to slow as the temperature of the press fell. Additional DSC scans were performed using an equivalent cooling rate of 1.5°C/min. At this rate the onset of crystallization occurred at approximately T_c

TABLE II
Overall Averages and Standard Deviations of Thermal Properties for the PFA Films as a Function of Grade and Cooling Method

| Grade	Cooling Method	T_m (°C)	ΔH (J/g)	x_c
440HP	Ice quench	307 ± 1	23.9 ± 0.6	0.36 ± 0.02
	Press cool	315 ± 1	27.5 ± 0.8	0.41 ± 0.01
450HP	Ice quench	308 ± 1	20.6 ± 1.0	0.31 ± 0.02
	Press cool	314 ± 1	26.4 ± 1.3	0.40 ± 0.02
451HPJ	Ice quench	310 ± 1	22.0 ± 1.8	0.33 ± 0.03
	Press cool	317 ± 1	28.8 ± 2.1	0.43 ± 0.03
950HP+	Ice quench	291 ± 1	13.0 ± 1.8	0.19 ± 0.03
	Press cool	$283 \pm 1/304 \pm 1$	18.0 ± 2.6	0.27 ± 0.04
951HP+	Ice quench	$289 \pm 1/323 \pm 2$	$3.2 \pm 0.7/13.5 \pm 1.6$	0.25 ± 0.11
	Press cool	$289 \pm 1/328 \pm 1$	$7.5 \pm 0.9/16.3 \pm 0.3$	0.36 ± 0.02

= 300°C. By analyzing the cooling curve, it was surmised that the PFA began to crystallize after the first 30–45 min of cooling. It took about 6 h for the press temperature to drop below the glass transition temperature (T_g) of the PFA (approximately T_g (80°C). Since crystallization only occurs between T_c and T_g, the time available for the PFA to crystallize during press cooling was about 6 h.

For a given cooling condition, the 440HP and 450HP PFAs had similar melting behavior and crystallinity. With higher comonomer content, the 950HP+ had a lower crystalline fraction than 440HP or 450HP. In Figure 1, 950HP+ shows a lower melting temperature and has broader melting transition than 450HP. 451HPJ and 951HP+ both contained PTFE and accordingly showed two melting peaks. These two PTFE filled grades showed higher crystallinity than their unfilled counterparts. The melting peaks of the 451HPJ were difficult to differentiate because they overlapped and our software was not capable of deconvoluting them. Thus, accurate estimates of the relative amount of PTFE from DSC measurements alone were difficult. Hence, the fraction of PTFE in the 451HP was measured by infrared (IR) spectroscopy along with the 951HP+.

Figure 2 shows two FTIR spectra of PFA grades with different comonomer. Two distinctive peaks from PPVE and PEVE at 995 and 1090 cm^{-1}, respectively, can be seen easily. The internal reference peak at 2365 cm^{-1} is from a combination mode of PTFE backbone and is rather insensitive to small changes of comonomer amount. This peak depends only on the thickness of the sample and therefore can be used to normalize spectra from samples with slightly different thicknesses.
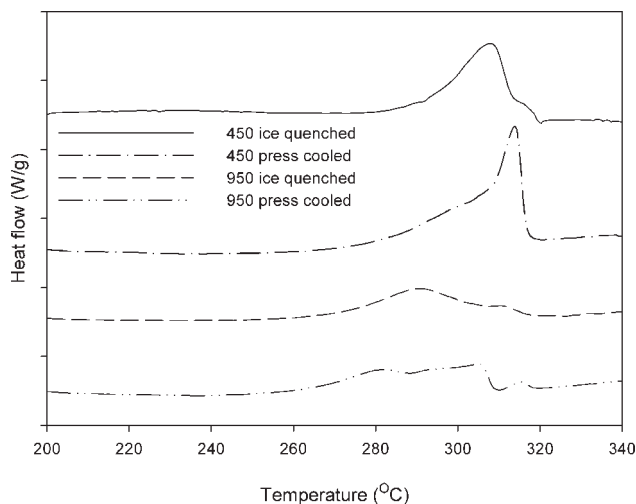
Figure 1 DSC thermograms from two different grades of PFA molded using two different cooling methods. The curves are from the first heating cycle and are normalized with the sample weight. The tick spacing of the vertical axis represent 0.2 W/g.
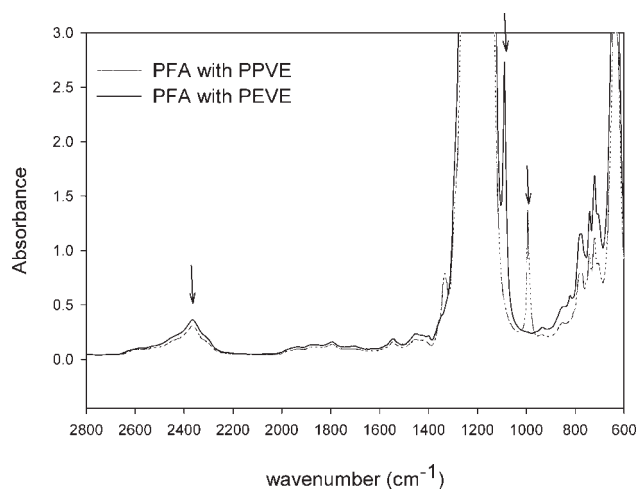
Figure 2 FTIR spectra of two grades of PFA having PPVE and PEVE as comonomer.

Table III lists the PAVE comonomer type, FTIR peak intensities, intensity ratios as well as mass and molar comonomer fractions of the various PFAs. FTIR showed that the comonomer in the 950HP+ and 951HP+ was PEVE, all other contained PPVE comonomer. The PPVE comonomer content in the 440 HP and 450HP was estimated to be approximately 4% by mass. The 950HP+ had the highest comonomer content, nearly 10%. As compared to the 450HP and 950HP+, the comonomer content in the 451HPJ and 951HP+ was diluted due to the presence of the PTFE filler (which contains no comonomer). Our estimates suggest that 451HPJ contains about 12% PTFE and 951HP+ contains about 30% PTFE.

Figure 3 shows the downstream pressure (Δp_l) with the passage of time for oxygen permeating through a 0.45 mm press cooled 440HP PFA film from three separate trials, where the applied upstream pressures were Δp = 2.0, 4.1, and 6.0 atm. Initially, Δp_l remained constant. After about 30 min, oxygen broke through and Δp_l began to rise with time, reaching steady state after several hours. Permeation rates were proportional to the applied upstream pressure.

The downstream pressures (Δp_l) from Figure 3 were converted to gas volumes at STP [eq. (6)] and then plotted in Figure 4 as V $B/A\cdot\Delta p$ versus t according to eq. (7). The points are experimental data and the solid line represents linear regression from longer times. The slope of the line in Figure 2 is equal to the permeability coefficient (P), which for this film, has a value of P = 2.4 × 10^{-10} cm^3 cm/ cm^2 s cmHg. The break-through times (t_b) were estimated from the intersection of two lines—the first is defined by the permeability coefficient and the second is a zero slope dashed line passing through the initial Δp_l at t = 0 s. For the data in Figure 4, t_b =

TABLE III
PAVE Comonomer Type, Peak Intensities, Intensity Ratios as well as Mass and Molar Comonomer Fractions of the Various PFAs

Grade	Co-monomer	I_{PAVE}	I_{ref}	I_{PAVE}/I_{ref}	x_{PAVE}	v_{PAVE}
440HP	PPVE	1.362	0.306	4.451	4.18	1.62
450HP	PPVE	2.048	0.489	4.188	3.94	1.52
451HPJ	PPVE	1.796	0.489	3.673	3.45	1.33
950HP+	PEVE	2.188	0.306	7.150	9.51	4.64
951HP+	PEVE	2.221	0.443	5.014	6.67	3.20

2000 s (about 33 min) corresponding to a diffusion coefficient of $D = 15 \times 10^{-8}$ cm^2/s. From the quotient of P and D [eq. (8)], the solubility coefficient was estimated as $S = 1.6 \times 10^{-3}$ cm^3/cm^3 cmHg. Data from the various pressures gave unique values of P, D, and S. Other measurements behaved similarly, but P, D, and S values depended on grade, cooling method, and gas.

Table IV lists P, D, and S values for hydrogen, oxygen and nitrogen gas permeating through ice quenched and press cooled 440HP PFA. These data are typical for a given grade and process. Hydrogen diffused much faster than oxygen. On the other hand, oxygen diffused a bit faster than nitrogen. Solubility of these gases in PFA was relatively low, with oxygen being only slightly more soluble than nitrogen or hydrogen.

Table V lists P, D, and S values for hydrogen gas permeating through various PFA films. In comparing 440HP and 450HP, both have the same molecular architecture (same comonomer type, comonomer content, and end groups) and differ only in their molecular mass or chain length. The 450HP with its longer chains has higher viscosity and lower MFR than 440HP. While dramatically affecting properties such as viscosity and fatigue life, the total length of the polymer chains generally does not affect mor-

phology very much. In the act of permeating through a polymeric material, the small molecules associated with gases and simple liquids slip through ephemeral holes created by the interaction of short segments of adjacent polymer chains. Indeed, in comparing 440HP to 450HP, the P and D values were nearly identical. P values for 450HP were a just bit larger, perhaps due to its longer chains retarding the development of crystallinity slightly more than its shorter chain equivalent, 440HP.

The 950HP+ has higher comonomer content than the 440HP or 450HP. The higher concentration of side chains causes greater disruption along main chain axis, which further reduces the ability of the 950HP+ PFA chains to pack tightly and form crystals. Consequently, the 950HP+ had less crystallinity than the 440HP or 450HP. Because amorphous regions are less dense than crystalline domains due to their more chaotic molecular organization, this looser structure allows molecules to permeate more readily. With a higher proportion of amorphous content, 950HP+ had slightly less permeation resistance than 440HP or 450HP, Table V.

Both 451HPJ and 951HP+ contain PTFE filler. PTFE usually exhibits much higher crystallinity than PFA (approximately 60% for PTFE versus 20–40% for PFA). Thus, adding PTFE to PFA generally
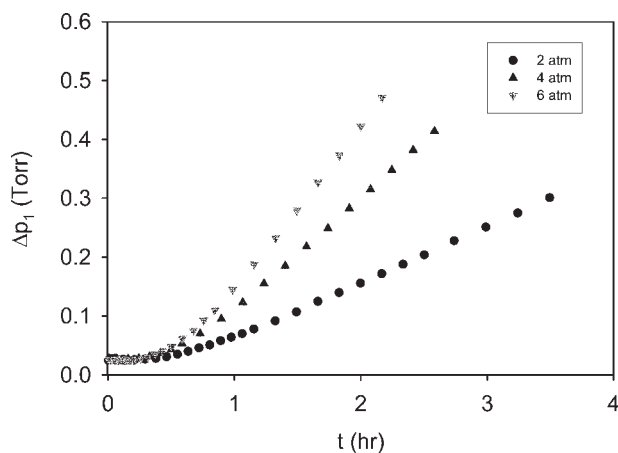
Figure 3 Downstream pressure (Δp_l) versus time (t) for oxygen permeating through a 0.45 mm press cooled 440HP PFA film from three separate trials, where the applied upstream pressures were $\Delta p = 2.0$, 4.1, and 6.0 atm.
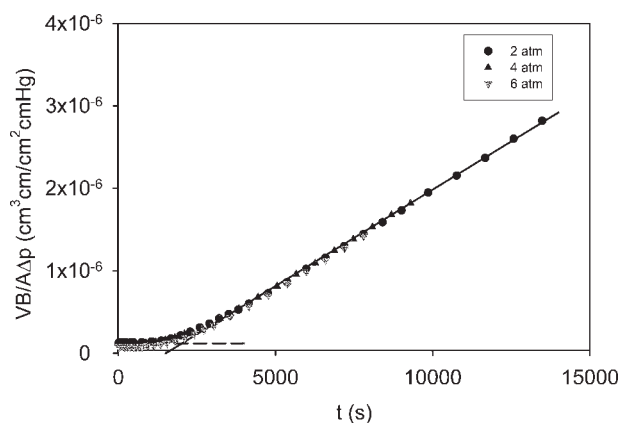
Figure 4 A plot of $V B/A \cdot \Delta p$ versus time (t) for oxygen permeating through a 0.45 mm press cooled PFA film under three different applied upstream pressures: $\Delta p = 2.0$, 4.1, and 6.0 atm.

TABLE IV
Permeability Coefficients (P), Diffusion Coefficients (D), and Solubility Coefficients (S) of the Various Gases Through 440HP PFA at 25°C

Permeant	Cooling method	P (10^{-10} cm^3 cm/cm^2 s cmHg)	D (10^{-8} cm^2/s)	S (10^{-3} cm^3/ cm^3 cmHg)
Hydrogen (H$_2$)	Ice quench	16 ± 0.1	230 ± 30	0.70 ± 0.11
	Press cool	6.8 ± 0.1	150 ± 15	0.45 ± 0.04
Oxygen (O$_2$)	Ice quench	5.7 ± 0.01	24 ± 0.7	2.4 ± 0.07
	Press cool	2.4 ± 0.1	15 ± 1	1.6 ± 0.1
Nitrogen (N$_2$)	Ice quench	1.94 ± 0.01	11.8 ± 0.6	1.7 ± 0.1
	Press cool	0.81 ± 0.01	7.8 ± 0.4	1.1 ± 0.1

boosts crystalline content. Furthermore, the addition of PTFE powder to PFA is believed to act as a nucleation site for the formation of crystals, thereby increasing not only the overall cystallinity, but also the number of crystalline domains. The 12% PTFE in 451HPJ would be expected to boost its crystallinity by 10% as compared with 450HP and reduce permeation. Indeed, the crystallinity and permeation resistance of 451HPJ were about 10% greater than 450HP. With 30% PTFE, 951HP+ had the commensurate amount of crystallinity relative to 950HP+, 36% versus 27%. Although the addition of PTFE caused a proportionate increase in crystallinity, the permeation resistance did not scale accordingly. Slow cooled 951HP+ specimens had nearly twice the permeation resistance of 950HP+ specimens, Table V. Thus it seems that variation in permeation cannot be explained solely by crystalline content alone. Differences in crystal morphology probably also played a role.

Processing had the greatest influence on the permeation resistance of the various PFAs. For each grade shown in Table V, allowing the specimens to cool slowly in the press versus quenching in an ice bath doubled their hydrogen permeation resistance. The two other gases behaved similarly to hydrogen: chain length had no appreciable influence on permeation resistance; higher comonomer content reduced crystallinity thereby increasing their permeation slightly; the addition of PTFE filler reduced their permeation; finally, processing had a dramatic influence on their permeability.

CONCLUSIONS

Permeability, diffusion, and solubility coefficients were measured for a variety of compression molded PFA films and were found to be independent of applied upstream pressure and thickness. Generally, films allowed to cool in the press overnight produced higher crystallinity and greater permeation resistance than those that were quickly quenched in ice water. For a given cooling method, chain length (e.g., 440HP versus 450HP) had no appreciable affect on the permeation resistance. On the other hand, PFA grades with increased comonomer content (e.g., 950HP+) appeared to have slightly diminished permeation resistance whereas grades with PTFE filler (e.g., 451HP and 951HP+) had better permeation resistance. The influence of the process (cooling method) was arguably more important in determining permeation resistance than polymer chain architecture structure. Slower cooling rates associated with the press-cooled specimens generally led to greater crystallinity and better permeation resistance. The permeation resistance of the press-cooled specimens generally was about twice that of the ice water quenched specimens.

TABLE V
Overall Averages of Permeability Coefficients (P), Diffusion Coefficients (D), and Solubility Coefficients (S) of the Hydrogen Gas at 25°C for the Various PFA Films

Grade	Cooling method	P (10^{-10} cm^3 cm/cm^2 s cmHg)	D (10^{-8} cm^2/s)	S (10^{-3} cm^3/cm^3 cmHg)
440HP	Ice quench	16 ± 0.1	230 ± 30	0.70 ± 0.11
	Press cool	6.8 ± 0.1	150 ± 10	0.45 ± 0.04
450HP	Ice quench	17 ± 1	270 ± 20	0.63 ± 0.04
	Press cool	8.1 ± 0.1	150 ± 10	0.57 ± 0.06
451HPJ	Ice quench	18 ± 1	250 ± 40	0.75 ± 0.11
	Press cool	7.7 ± 0.1	135 ± 20	0.58 ± 0.06
950HP+	Ice quench	17 ± 1	260 ± 20	0.71 ± 0.01
	Press cool	10 ± 1	170 ± 30	0.62 ± 0.14
951HP+	Ice quench	15 ± 1	230 ± 30	0.66 ± 0.08
	Press cool	4.7 ± 0.1	74 ± 5	0.63 ± 0.01

References

1. Khaladkar, P. R. In Modern Fluoropolymers; Scheirs, J., Ed.; Wiley: New York, 1997; pp 311–326.
2. Extrand, C. W. J Fluorine Chem 2003, 122, 121–124.
3. Goodman, J. B.; Andrews, S. J. Solid State Technol 1990, 33, 65–68.
4. Goodman, J. B.; Van Sickle, P. M. Microcontamination 1991, 9, 21–26.
5. Kerbow, D. L.; Sperati, C. A. In Polymer Handbook, 4th ed.; Brandrup, J., Immergut, E. H., Grulke, E. A., Eds. Wiley: New York, 1999; pp V/31–V/48.
6. Giacobbe, F. W. J Appl Polym Sci 1990, 39, 1121–1132.
7. Giacobbe, F. W. J Appl Polym Sci 1991, 42, 2361–2364.
8. Giacobbe, F. W. J Appl Polym Sci 1992, 466, 1113.
9. Pauly, S. In Polymer Handbook, 4th ed.; Brandrup, J., Immergut, E. H., Grulke, E. A., Eds. Wiley: New York, 1999; pp VI/543–VI/569.
10. Extrand, C. W.; Monson, L. J Appl Polym Sci 2006, 100, 3.
11. Prabhakar, R. S.; De Angelis, M. G.; Sarti, G. C.; Freeman, B. D.; Coughlin, M. C. Macromolecules 2005, 38, 7043.
12. De Angelis, M. G.; Sarti, G. C.; Sanguineti, A.; Maccone, P. J Polym Sci Part B: Polym Phys 2004, 42, 1987–2006.
13. Aminabhavi, T. M.; Naidu, B. V. K. J Appl Polym Sci 2004, 92, 991–996.
14. Kerbow, D. L. U.S. Pat 5,780,882 (1998).
15. Daynes, H. A. Proc R Soc (London) 1920, A97, 286–307.
16. Standard Test Method for Determining Gas Permeability Characteristics of Plastic Film and Sheeting (D1434-82). ASTM: West Conshohocken, PA, 1998.
17. Runt, J. P. In Encyclopedia of Polymer Science and Engineering, 2nd ed.; Mark, H. F., Kroschwitz, J. I., Eds. Wiley: New York, 1986; Vol. 4, pp 482–519.
18. Osswald, T. A.; Menges, G. Materials Science of Polymers for Engineers. Hanser: New York, 1995.
19. Crank, J. The Mathematics of Diffusion. Oxford University Press: London, 1970.